Molecular Crystals and Liquid Crystals

Publication details, including instructions for authors and subscription information:
http://www.tandfonline.com/loi/gmcl20

Carrier Transport Mechanisms of Organic Light-Emitting Devices with an Ultra Thin 5,6,11,12-tetraphenylnaphthacene Layer Embedded in a Hole Transport Layer or/and an Emitting Layer

B. C. Kwack [a], D. C. Choo [a], T. W. Kim [a b], J. H. Seo [c], J. H. Park [c] & Y. K. Kim [c]

[a] Research Institute of Information Display, Department of Information Display Engineering, Hanyang University, Seoul, Korea

[b] Division of Electronics and Computer Engineering, Hanyang University, Seoul, Korea

[c] Department of Information Display Engineering & COMID, Hong-ik University, Seoul, Korea

Version of record first published: 22 Jul 2010

Mol. Cryst. Liq. Cryst., Vol. 498, pp. 249–257, 2009

ISSN: 1542-1406 print/1563-5287 online
DOI: 10.1080/15421400802619297

Taylor & Francis
Taylor & Francis Group

Carrier Transport Mechanisms of Organic Light-Emitting Devices with an Ultra Thin 5,6,11,12-tetraphenylnaphthacene Layer Embedded in a Hole Transport Layer or/and an Emitting Layer

B. C. Kwack[1], D. C. Choo[1], T. W. Kim[1,2], J. H. Seo[3], J. H. Park[3], and Y. K. Kim[3]

[1]Research Institute of Information Display, Department of Information Display Engineering, Hanyang University, Seoul, Korea
[2]Division of Electronics and Computer Engineering, Hanyang University, Seoul, Korea
[3]Department of Information Display Engineering & COMID, Hong-ik University, Seoul, Korea

While the current density of the organic light-emitting devices (OLEDs) with 5,6,11,12-tetraphenylnaphthacene (rubrene) layers in both the hole transport layer (HTL) and the emitting layer (EML) was lower than those of the OLEDs without a rubrene layer or with a rubrene layer in only a HTL or an EML, the luminance efficiency of the OLEDs with rubrene layers in both the HTL and the EML were significantly enhanced. While the rubrene layer in the HTL acting as a hole trap decreased the hole mobility of the HTL, the rubrene layer in the EML acting as an emitting site increased the luminance.

Keywords: carrier transport; emitting site; high efficiency, hole trap; organic light-emitting devices; ultra thin layer

I. INTRODUCTION

Organic light-emitting devices (OLEDs) have emerged as promising candidates for potential applications in full-color flat-panel displays with a large area [1–3]. OLEDs have become particularly attractive

This work was supported by the Korea Science and Engineering Foundation (KOSEF) grant funded by the Korea government (MEST) (No. R0A-2007-000-20044-0).

Address correspondence to Prof. Tae Whan Kim, Division of Electronics and Computer Engineering, Hanyang University, 17 Haengdang-dong, Seongdong-gu, Seoul 133-791, Korea (ROK). E-mail: twk@hanyang.ac.kr

due to their unique advantages of low driving voltage, low power consumption, high contrast, wide viewing angle, low cost, and fast response [4–6]. Moderate controls of carrier injection and transport for efficient carrier recombination and balance of the electrons and the holes are very important for fabricating high-efficiency OLEDs [7,9]. Even though many studies on the efficiency enhancement of OLEDs utilizing various structures, such as a doped layer in the host mixed structure [10], a graded mixed structure [11], a multiple-quantum-well structure [12,13], an organic-inorganic hybrid structure [14], and a stacked structure [15], have been performed, studies on carrier transport mechanisms in OLEDs without or with an ultra thin organic layer embedded into a hole transport layer (HTL) or/and an emitting layer (EML) have not yet been carried out. Furthermore, studies of carrier transport mechanisms of OLEDs with an ultra thin 5,6,11,12-tetraphenylnaphthacene (rubrene) layer embedded in a HTL or/and an EML are necessary for achieving high efficiency of OLEDs.

This paper reports data for the carrier transport mechanism of OLEDs with an ultra thin rubrene layer embedded in a HTL or/and an EML fabricated by using organic molecular beam deposition (OMBD). Current density-voltage, luminance-voltage, and electroluminescence (EL) measurements were carried out to investigate electrical and optical properties of the OLEDs with an ultra thin rubrene layer embedded in a HTL or/and an EML. Carrier transport mechanisms of OLEDs with an ultra thin rubrene layer embedded in a HTL or/and an EML are described on the basis of the experimental results.

II. EXPERIMENTAL DETAILS

The sheet resistivity of the indium-tin-oxide (ITO) thin films on glass substrates used in this study was 30 Ω/square. The ITO substrates were cleaned by using acetone and methanol at 60°C for 5 min and were rinsed in de-ionized water thoroughly. The chemically cleaned ITO substrates were then dried by using N_2 gas with a purity of 99.9999%. The three kinds of samples used in this study were fabricated on ITO thin films coated on glass substrates by using OMBD with effusion cells and shutters. The OLED structures used in this study are summarized in Table 1, and the corresponding schematic energy band diagrams of the fabricated OLEDs without and with an ultra thin rubrene layer inserted HTL or EML are shown in Figure 1. Devices II, III, and IV excepting reference device I contain a rubrene layer, and the quantity of the rubrene existing in devices II, III, and IV is same. While devices II and III contain a 2 nm-rubrene layer in the HTL or the EML, respectively, device IV contains double 1 nm-rubrene layers in both the

TABLE 1 The Structure of the OLEDs

	Device structure
Device I	ITO/NPB (40 nm)/DPVBi (45 nm)/Alq_3 (30 nm)/Liq (2 nm)/Al
Device II	ITO/NPB (33 nm)/Rubrene (2 nm)/NPB (5 nm)/DPVBi (45 nm)/Alq_3 (30 nm)/Liq (2 nm)/Al
Device III	ITO/NPB (40 nm)/DPVBi (5 nm)/Rubrene (2 nm)/DPVBi (38 nm)/Alq_3 (30 nm)/Liq (2 nm)/Al
Device IV	ITO/NPB (34 nm)/Rubrene (1 nm)/NPB (5 nm)/DPVBi (5 nm)/Rubrene (1 nm)/DPVBi (39 nm)/Alq_3 (30 nm)/ Liq (2 nm)/Al

HTL and the EML. The organic layers were deposited at a substrate temperature of 27°C and a system pressure of 5×10^{-6} Torr. The deposition rates of the organic layers and the metal layers were approximately 1 and 10 Å/s, respectively. The deposition rates were controlled by using a quartz crystal monitor. The current density-voltage characteristics of the OLEDs were measured on a programmable electrometer with built-in current and voltage measurement units (model 236, Keithely). The brightness was measured by using a brightness meter, chroma meter CS-100A (Minolta).

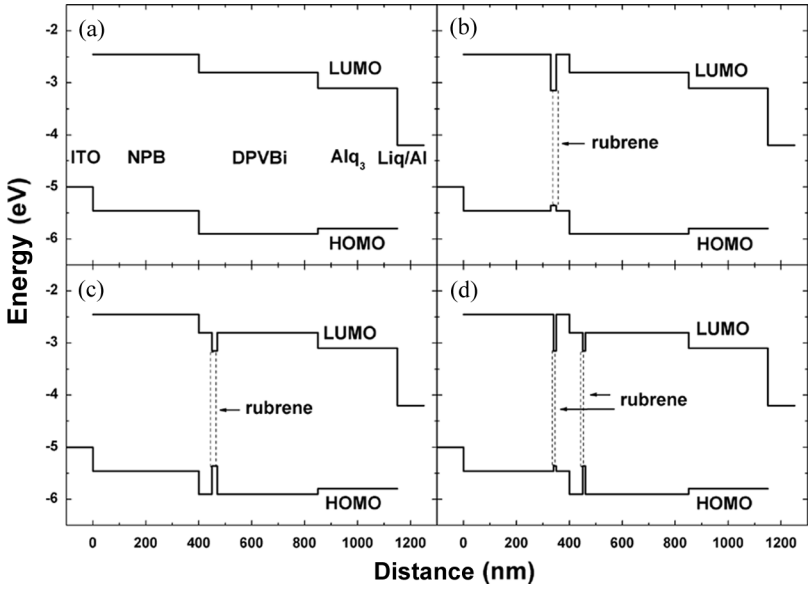

FIGURE 1 Schematic energy band diagrams for the OLEDs of devices I, II, III, and IV.

III. RESULTS AND DISCUSSION

Figure 1 shows schematic energy band diagrams for the OLEDs of devices I, II, III, and IV. The highest occupied molecular orbital (HOMO) and the lowest unoccupied molecular orbital (LUMO) levels of the 4,4′-bis(2,2-diphenylvinyl)biphenyl (DPVBi) are −5.9 and −2.8 eV, respectively [16], and the HOMO and the LUMO levels of the N,N′-bis(1-naphthyl)-N,N′-diphenyl-1,1′-biphenyl-4,4′-diamine (NPB) layer, as obtained by using cyclic voltammetry, are −5.46 and −2.45 eV, respectively [17]. The HOMO and the LUMO levels of the rubrene layer are −5.36 and −3.15 eV, respectively [18]. Because the HOMO level of the rubrene layer is smaller than those of the NPB and the DPVBi layers, the rubrene layer acts as a hole trapping layer. The rubrene layer acts also an electron trapping layer excepting the difference in the depths of the hole and the electron trapping layer. Because the trapped electrons and holes form the exciton due to radiative recombination, the rubrene layer serves as the hole and the electron trapping layers acts as an emission site.

Figure 2 shows current densities as functions of the applied voltage for OLEDs of devices I, II, III, and IV. The current densities as functions of the applied voltage for OLEDs of devices I, II, and III show almost similar behavior. The thickness of the rubrene layer embedded in the HTL or the EML is too thin to affect the total current density in the OLEDs. Even though the current densities of devices II and III are slightly larger than that of device I, the existence of the ultra thin rubrene layer is not enough to distinguish the differences of current densities for devices II and III in comparison with that for device I. Because the electron and hole injections in device IV are suppressed by the trapped charges in the rubrene layers, the current density of device IV with two rubrene layers is the lowest among the four kinds of devices.

Figure 3 shows that the luminances as functions of the applied voltage for OLEDs of devices I, II, III, and IV. While the luminance of devices III at low voltage is larger than those of other devices, the luminance of device III at high voltage is smaller than those of other devices. The luminance enhancement of device III at low voltage is attributed to the existence of the large luminescence region in the trap layer, and the luminescence region in the trap layer shifts to a different region with increasing applied voltage, resulting in a decrease in the luminance of device III.

Figure 4 shows that the luminance efficiencies as functions of the current density for OLEDs of devices I, II, III, and IV. The luminance efficiency of device IV with two inserted rebrene layers is larger than those of other devices with and without one inserted rubrene layer.

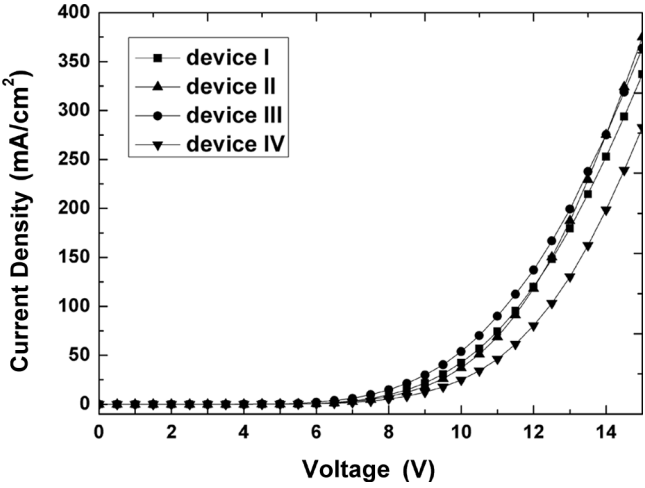

FIGURE 2 Current densities as functions of the applied voltage for OLEDs of devices I, II, III, and IV. Filled rectangles, upright triangles, circles, and inverted triangles represents the OLEDs of devices I, II, III, and IV, respectively.

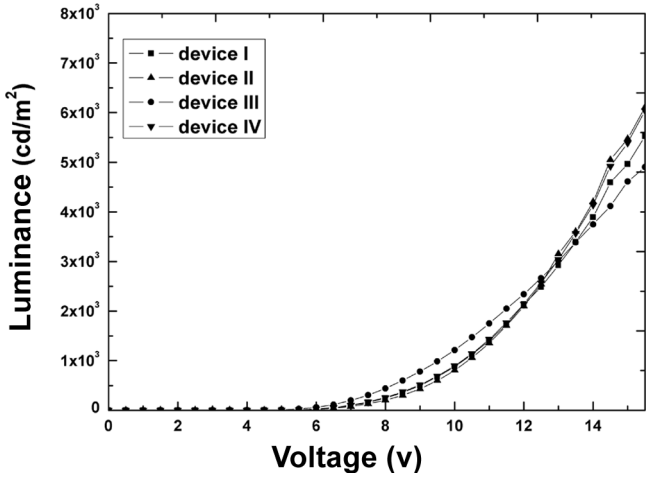

FIGURE 3 Luminance as functions of the applied voltage for OLEDs of devices I, II, III, and IV. Filled rectangles, upright triangles, circles, and inverted triangles represents the OLEDs of devices I, II, III, and IV, respectively.

When the same magnitude of the trap layer is used as a inserted layer, the luminance efficiency of the OLEDs increases with increasing a number of the inserted rubrene layer resulting from the decrease in the hole mobility. The luminous efficiency of device IV is the highest among the devices used in this work. The maximum luminous efficiencies of devices I, II, III, and IV are 3.2, 2.5, 3.4, and 5.7 cd/A, respectively. The efficiency enhancement in the OLEDs is dominantly related to the number of the rubrene layer corresponding to the number of the heterointerfaces in the OLEDs rather than the quantity of the inserted rubrene.

Figure 5 shows the EL spectra at various applied voltages for OLEDs of devices (a) I, II, (b) III, and (c) IV. The emission peaks at around 465 and 555 nm for devices are attributed to the DPVBi EML and the inserted rubrene layer. The EL spectra for devices I and II show the same shape, as shown in Fig. 5(a), regardless of applied voltages. The same shape of the EL spectra for devices I and II indicate that the inserted rubrene layer of device II acts as only a trap layer. Even though device II contains an ultra thin rubrene layer embedded in the NPB HTL, the emission spectra are not affected by the inserted layer, as shown in Figure 5(a). The EL spectra for devices III and IV are varied by changing applied voltage. The inserted

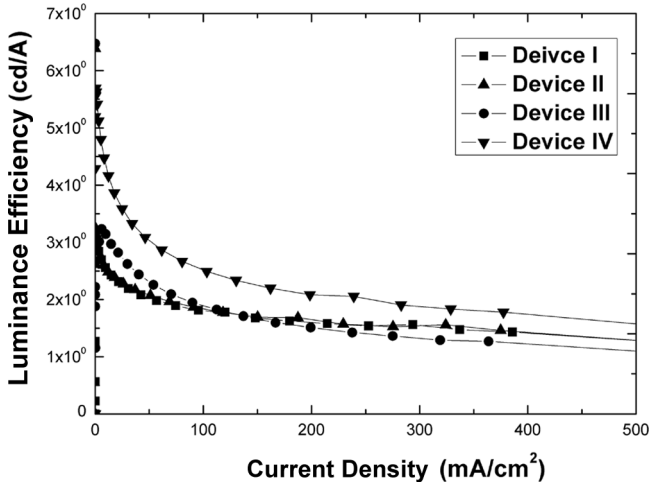

FIGURE 4 Luminance efficiency as functions of the current density for OLEDs of devices I, II, III, and IV. Filled rectangles, upright triangles, circles, and inverted triangles represents the OLEDs of devices I, II, III, and IV, respectively.

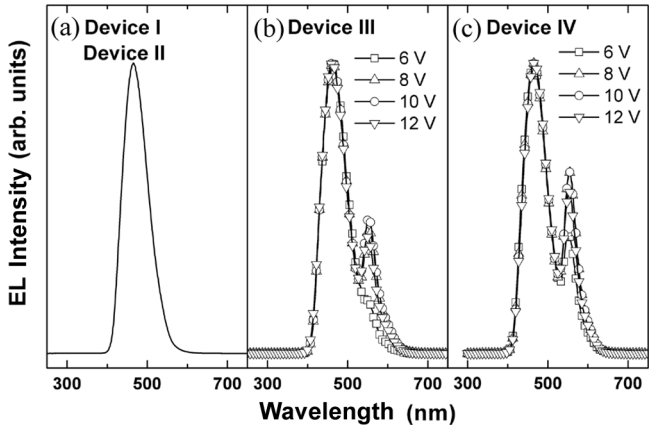

FIGURE 5 Normalized electroluminescence spectra at various applied voltages for OLEDs of devices (a) I and II, (b) III, and (c) IV.

rubrene layer of device III in the EML acts as a hole trapping layer and an EML. The EL spectra for device III shows two emission peaks at around 465 and 555 nm. The intensity related to the rubrene peak at 555 nm for device III increases with increasing applied voltage up to 11 V, and the corresponding peak intensity decreases with increasing applied voltage above 11 V. Even though the EL spectrum for device IV shows similar behavior to that for device III, the maximum luminescence intensity related to the rubrene peak for device IV is 8 V, which is smaller than the corresponding voltage for device III.

Figure 6 show the schematic diagrams describing carrier transport mechanisms for OLEDs of devices III and IV. The EMLs of devices III and IV consist of three different regions, denoted by 1, 2, and 3. The carrier transport mechanisms for OLEDs of devices III and IV are described on the results of the EL spectra shown in Figure 5. The carrier transport properties of devices III with a rubrene layer embedded in the EML and IV with rubrene layers embedded in the HTL and EML under low voltages are dominantly affected by the existence of the shallow traps at the organic layers. The number of the electron existing in the region 1 of device III under low voltages is not affected by the trap layer that in the region 2 of device III is significantly affected by the trap layer. Therefore, the number of the electron in the region 2 of device III increases with increasing applied voltage up to a critical voltage, resulting in the fully occupation of the number of the electron in the shallow traps. While the number of the occupied electron in the rubrene layer of device III increases with increasing

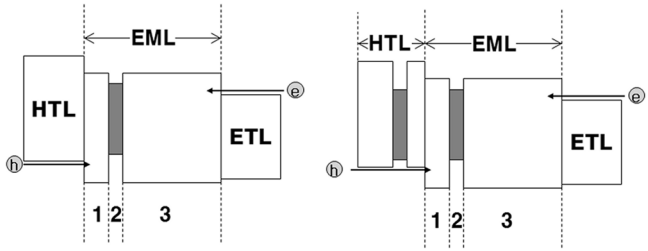

FIGURE 6 Schematic diagrams describing carrier transport mechanisms for OLEDs of devices III and IV.

applied voltage up to 11 V, resulting in an increase in the luminescence intensity related to the rubrene layer, the number of the electron in the region 1 of device III increases with increasing applied voltage about 11 V, resulting in a decrease in the luminescence intensity related to the rubrene layer. These results are in reasonable agreement with the EL spectra shown in Figure 5(b). The transition voltage of the EL peak intensity related to the rubrene layer for device IV is smaller than that for device II. The decrease in the transition applied voltage for device IV in comparison with device III is attributed to the existence of the shallow traps in both the HTL and the EML. Because the thicknesses of the rubrene trap layers in device IV are thinner than that of the trap layer in device III, the shallow traps existing in the device IV at lower voltages are fully occupied by the electron, resulting in the decrease of the transition voltage.

IV. SUMMARY AND CONCLUSIONS

The carrier transport mechanisms of OLEDs utilizing an ultra thin rubrene layer embedded in an NPB HTL or/and a DPVBi EML were investigated. The current density of the OLEDs with rubrene layers embedded in the HTL and the EML was lower than those of the OLEDs without a rubrene layer or with a rubrene layer in only the HTL or only the EML. The luminance efficiency of the OLEDs with rubrene layers embedded in both the HTL and the EML were significantly enhanced in comparison with those with a rubrene layer embedded in only the HTL or only the EML. Because the rubrene layer embedded in the HTL dominantly acted as hole traps, the hole mobility of the HTL decreased due to an existence of the hole traps. When the rubrene layer embedded in the EML dominantly acted as

an emitting site, the luminance of OLEDs increased due to an increase of the emitting sites resulting from the existence of the rubrene layer. The EL spectra for devices with a rubrene layer embedded in only the EML and rubrene layers embedded in both the HTL and the EML showed that the peak intensities related to the rubrene layer were changed with varying applied voltage. Carrier transport mechanisms of the OLEDs with an ultra thin rubrene layer embedded in the HTL or/and EML are described on the basis of the experimental results. These results can help to improve understanding of the carrier transport mechanisms of the OLEDs with rubrene layers embedded in the HTL or/and the EML.

REFERENCES

[1] Shen, Z., Burrows, P. E., Bulovic, V., Forrest, S. R., & Thompson, M. E. (1997). *Science*, *276*, 2009.
[2] Chen, S.-Y., Chu, T.-Y., Chen, J.-F., Su, C.-Y., & Chen, C. H. (2006). *Appl. Phys. Lett.*, *89*, 053518.
[3] Kanno, H., Giebink, N. C., Sun, Y., & Forrest, S. R., (2006). *Appl. Phys. Lett.*, *89*, 203503.
[4] Baldo, M. A., O'Brien, D. F., You, Y., Shoustikov, A., Sibley, S., Thompson, M. E., & Forrest, S. R. (1998). *Nature*, *395*, 151.
[5] Adachi, C., Baldo, M. A., & Forrest, S. R. (2000). *Appl. Phys. Lett.*, *77*, 904.
[6] Young, R. H., Tang, C. W., & Marchetti, A. P. (2002). *Appl. Phys. Lett.*, *80*, 874.
[7] Ma, D., Lee, C. S., Lee, S. T., & Hung, L. S. (2002). *Appl. Phys. Lett.*, *80*, 3641.
[8] Okumoto, K., Kanno, H., Hamada, Y., Takahashi, H., & Shibata, K. (2006). *Appl. Phys. Lett.*, *89*, 013502.
[9] Yoon, Y. B., Bang, H. S., Kim, T. W., Kim, J. H., Seo, J. H., Kim, Y. K. (2006). *Molecular Crystals and Liquid Crystals*, *459*, 283.
[10] Choong, V. E., Shi, S., Curless, J., Shieh, C.-L., Lee, H.-C., Shen, J., & Yang, J. (1999). *Appl. Phys. Lett.*, *75*, 172.
[11] Chwang, A. B., Kwong, R. C., & Brown, J. J. (2002). *Appl. Phys. Lett.*, *80*, 725.
[12] Qiu, Y., Gao, Y., Wang, L., Wei, P., Duan, L., Zhang, D., & Dong, G. (2002). *Appl. Phys. Lett.*, *81*, 3540.
[13] Choo, D. C., Yoon, Y. B., Lee, D. U., Kim, T. W., Lee, H. K., Kim, Y. K. (2007). *Molecular Crystals and Liquid Crystals*, *470*, 269.
[14] Coe, S., Woo, W.-K., Bawendi, M., & Bulović, V. (2002). *Nature*, *420*, 800.
[15] Sun, J. X., Zhu, X. L., Peng, H. J., Wong, M., & Kwok, H. S. (2005). *Appl. Phys. Lett.*, *87*, 93504.
[16] Zheng, X. Y., Zhu, W. Q., Wu, Y. Z., Jiang, X. Y., Sun, R. G., Zhang, Z. L., & Xu, S. H. (2003). *Displays*, *24*, 121.
[17] Zhao, D.-W., Xu, Z., Zhang, F.-J., Song, S.-F., Zhao, S.-L., Wang, Y., Yuan, G.-C. Zhang, Y.-F., Xu, H.-H. (2007). *Appl. Surf. Sci.*, *253*, 4025.
[18] Hamada, Y., Kanno, H., Tsujioka, T., Takahashi, H., & Usuki, T. (1999). *Appl. Phys. Lett.*, *75*, 1682.